Inorganic Chemistry
Article

Inorg. Chem. **2009**, *48*, 9077–9084 **9077**
DOI: 10.1021/ic900190a

Multifunctional DNA Interactions of Ru−Pt Mixed Metal Supramolecular Complexes with Substituted Terpyridine Ligands

Avijita Jain,[†] Jing Wang,[†] Emily R. Mashack,[†] Brenda S. J. Winkel,[‡] and Karen J. Brewer*,[†]

[†]*Departments of Chemistry and,* and [‡]*Biological Sciences, Virginia Polytechnic Institute and State University, Blacksburg, Virginia 24061-0212*

Received January 29, 2009

The coupling of a light absorbing unit to a bioactive site allows for the development of supramolecules with multifunctional interactions with DNA. A series of mixed metal supramolecular complexes that couple a DNA-binding *cis*-$Pt^{II}Cl_2$ center to a ruthenium chromophore via a polyazine bridging ligand have been prepared, and their DNA interactions have been studied, $[(TL)RuCl(dpp)PtCl_2](PF_6)$ (TL = tpy (2,2′:6′,2″-terpyridine), MePhtpy (4′-(4-methylphenyl)-2,2′:6′,2″-terpyridine), or $^tBu_3$tpy (4,4′,4″-tri-*tert*-butyl-2,2′:6′,2″-terpyridine and dpp = 2,3-bis(2-pyridyl)pyrazine). This series provides for unique tridentate coordinated Ru(II) systems to photocleave DNA with preassociation with the DNA target via coordination of the Pt(II) center. Electronic absorption spectroscopy of the complexes displays intense ligand-based $\pi\rightarrow\pi^*$ transitions in the UV region and metal to ligand charge transfer (MLCT) transitions in the visible region. The Ru(dπ)→dpp(π^*) MLCT transitions occur at 545 nm, red-shifted relative to the 520 nm maxima for the monometallic synthons, $[(TL)RuCl(dpp)](PF_6)$. The title RuPt complexes display reversible $Ru^{II/III}$ oxidative couples at 1.10, 1.10, and 1.01 V vs Ag/AgCl for TL = tpy, MePhtpy, and $^tBu_3$tpy, respectively. The $TL^{0/-}$ reduction occurred at −1.43, −1.44, and −1.59 V vs Ag/AgCl for TL = tpy, MePhtpy, and $^tBu_3$tpy, respectively. These complexes display a $dpp^{0/-}$ couple (−0.50 −0.55, and −0.59 V) significantly shifted to positive potential relative to their monometallic synthons (−1.15, −1.16, and −1.22 V), consistent with the bridging coordination of the dpp ligand. Coupling of $(TL)Ru^{II}Cl(BL)$ subunit to a *cis*-$Pt^{II}Cl_2$ site provides for the application of photochemically inactive Ru^{II}(tpy)-based chromophores in DNA photocleavage applications. The $[(TL)RuCl(dpp)PtCl_2]^+$ complexes display covalent binding to DNA and photocleavage upon irradiation with visible light modulated by TL identity. The redox, spectroscopic, DNA-binding, and photocleavage properties of a series of supramolecular complexes are presented.

Introduction

Cisplatin, *cis*-$[Pt(NH_3)_2Cl_2]$ (*cis*-diamminedichloroplatinum-(II)), and its analogs are a class of widely used antitumor drugs. The antitumor activity of cisplatin derives from its binding to DNA and formation of covalent cross-links that inhibit both DNA replication and transcription.[1−4] Cisplatin is extensively used in the treatment of testicular, ovarian, bladder, lung, head, and neck carcinomas. Significant side effects, including nephrotoxicity, gastrointestinal toxicity, neurotoxicity, and ototoxicity, low water solubility, and drug resistance have limited the clinical applications of this drug. There has been a considerable interest in the development of cisplatin analogs with reduced toxicity and improved clinical efficacy.[5,6]

Ruthenium polyazine complexes have attracted the attention of researchers for decades.[7] These complexes possess highly versatile photophysical, photochemical, and redox properties and play an important role in electron and energy transfer processes. The prototypical ruthenium polyazine complex, $[Ru(bpy)_3]^{2+}$ (bpy = 2,2′-bipyridine), is well studied due to its long excited-state lifetime and interesting photophysical and redox properties.[7−9] Upon optical excitation at 450 nm, population of the Ru(dπ)→bpy(π^*) ^{1}MLCT occurs which populates the ^{3}MLCT state with unit efficiency. The ^{3}MLCT of $[Ru(bpy)_3]^{2+}$ is relatively long-lived and emissive

*To whom correspondence should be addressed. E-mail: kbrewer@vt.edu.

(1) Zang, C. X.; Lippard, S. *Curr. Opin.Chem. Biol.* **2003**, *7*, 481–489.
(2) Wong, E.; Giandomenico, C. M. *Chem. Rev.* **1999**, *99*, 2451–2466.
(3) Rosenberg, B.; Camp, V.; Kriagas, T. *Nature* **1965**, *205*, 698–699.
(4) Rosenberg, B.; L, V. C.; Trosko, J. E.; Mansour, V. H. *Nature* **1969**, *222*, 385–387.
(5) Hambley, T. *Dalton Trans.* **2001**, 2711–2718.
(6) Herman, A.; Tanski, J. M.; Tibbetts, M. F.; Anderson, C. M. *Inorg. Chem.* **2008**, *47*, 274–280.
(7) Kalyanasundaram, K. *Coord. Chem. Rev.* **1982**, *46*, 159–244.
(8) Juris, A.; Balzani, V.; Barigelletti, F.; Campagna, S.; Belser, P.; von Zelewsky, A. *Coord. Chem. Rev.* **1988**, *84*, 85–277.
(9) Balzani, V.; Juris, A.; Venturi, M.; Campagna, S.; Serroni, S. *Chem. Rev.* **1996**, *96*, 759–834.

Published on Web 09/09/2009

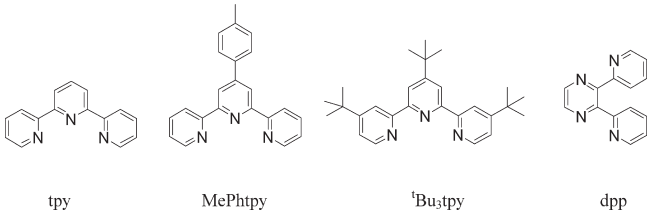

Figure 1. Polyazine ligands used in the study (tpy = 2,2′:6′,2″-terpyridine, MePhtpy = 4′-(4-methylphenyl)-2,2′:6′,2″-terpyridine, $^{t}Bu_3$tpy = 4,4′,4″-tri-*tert*-butyl-2,2′:6′,2″-terpyridine), dpp = 2,3-bis (2-pyridyl)pyrazine).

(λ_{max}^{em} = 605 nm, excited-state lifetime of the ^{3}MLCT, τ = 860 ns in acetonitrile).[10]

Applications of ruthenium(II) bis-tridentate polyazine light absorbers are more limited than the highly studied ruthenium(II) tris-bidentate polyazine chromophores. The complex, $[Ru(tpy)_2]^{2+}$ (tpy = 2,2′:6′,2″-terpyridine), exhibits less favorable photophysical properties than $[Ru(bpy)_3]^{2+}$, exhibiting a very short-lived ^{3}MLCT (0.25 ns in aqueous solution) excited state due to the thermal population of the ^{3}LF (ligand field) excited state.[11−14] The thermal accessibility of the ligand field state is due to the unfavorable bite angle for octahedral coordination associated with tpy-type ligands, lowering the energy of the ligand field state. The low-lying ^{3}LF state deactivates the normally emissive ^{3}MLCT state. The use of terpyridine ligands (Figure 1) provides the distinct advantage of allowing stereochemical control, eliminating the Δ and Λ isomeric mixtures, characteristic of tris-bidentate systems.

The photophysical properties of Ru(II) bis-tridentate polyazine metal complexes can be tuned by the introduction of various substituents on the terpyridine ligand.[15−22] Electron-withdrawing groups stabilize the lowest unoccupied molecular orbital (LUMO), while electron-donating groups destabilize the highest occupied molecular orbital (HOMO).[19,23] Stabilization of the lowest ^{3}MLCT state results in lower thermal population of the ^{3}LF state. Balzani and co-workers have reported both an increased excited-state lifetime and an emission quantum yield of $[Ru(tpy)_2]^{2+}$-type molecules upon incorporation of a methylphenyl group at the 4′ position of the terpyridine ring.[15] The 4′-methyl-sulphonyl substituted bis-terpyridine complexes have been shown to have lengthened room temperature luminescence lifetimes ($[Ru(MeSO_2\text{-}tpy)_2](PF_6)_2$, 25 ns; $[(MeSO_2\text{-}tpy)Ru(tpy-OH)](PF_6)_2$, 50 ns) due to the strong electron-withdrawing ability of the methylsulfonyl group.[19]

The DNA photocleavage activity of ruthenium polyazine complexes is well known.[24−26] These types of complexes have been shown to photocleave DNA via singlet oxygen ($^1O_2$) generation. The ^{3}MLCT state of these complexes undergoes energy transfer to molecular oxygen ($^3O_2$) to generate $^1O_2$, which reacts with DNA, cleaving the backbone.[24−26] Thummel and co-workers have reported that the complex, $[Ru(bpy)_2(DAP)]^{2+}$ (DAP = 1,12-diazaperylene), photocleaves DNA upon irradiation with visible light due to the formation of the $^1O_2$ species.[27] The lower excited-state lifetime of $[Ru(tpy)_2]^{2+}$ prevents its application in DNA photocleavage.[28,29]

Complexes incorporating a tpy ligand were reported to interact with DNA through electrostatic interaction, intercalation, and groove binding.[30−32] Turro and co-workers have recently reported the DNA photocleavage activity of $[Ru(tpy)(pydppz)]^{2+}$ (pydppz = 3-(pyrid-2′-yl)dipyrido(3,2-a:2′,3′-c]phenazine) in the presence of oxygen.[28] Thorp and co-workers have examined the DNA cleavage activity of $[Ru(tpy)(tmen)(OH_2)]^{2+}$ (tmen = *N*,*N*,*N*′,*N*′-tetramethylethylenediamine) by cyclic voltammetry.[26] The heteroleptic complexes, $[Ru(tpy)(PHBI)]^{2+}$ (PHBI = 2-(2-benzimidazole)-1,10-phenanthroline) and $[Ru(tpy)(PHNI)]^{2+}$ (PHNI = 2-(2-napthoimidazole)-1,10-phenanthroline), were reported to interact with DNA via electrostatic interaction and intercalation, respectively.[26] Recently, the $^1O_2$ generation and the DNA photocleavage ability of an aryl modified $[Ru(X\text{-}tpy)_2]^{2+}$ (X = 2-naphthyl, 1-pyrenyl, or 9-anthracenyl) complex has been reported.[33]

Mixed metal complexes, consisting of ruthenium light absorbers and a cisplatin unit, represent an emerging class of bioactive molecules of interest as anticancer agents. The enhanced covalent binding of mixed metal supramolecular complexes compared to cisplatin has been reported.[34,35] Complexes of the general formula $[(bpy)_2M(dpb)PtCl_2](PF_6)_2$ (where M = Ru and Os, dpb = 2,3-bis(2-pyridyl)benzoquinoxaline, bpy = 2,2′-bipyridine) bind with

(10) Durham, B.; Caspar, J. V.; Nagle, J. K.; Meyer, T. J. *J. Am. Chem. Soc.* **1982**, *104*, 4803–4810.
(11) Young, R. C.; Nagle, J. K.; Meyer, T. J.; Whitten, D. G. *J. Am. Chem. Soc.* **1978**, *100*, 4773–4778.
(12) Winkler, J. R.; Netzel, T. L.; Creutz, C.; Sutin, N. *J. Am. Chem. Soc.* **1987**, *109*, 2381–2392.
(13) Berger, R. M.; McMillin, D. R. *Inorg. Chem.* **1988**, *27*, 4245–4249.
(14) Kirchhoff, J. R.; McMillin, D. R.; Marnot, P. A.; Sauvage, J. P. *J. Am. Chem. Soc.* **1985**, *107*, 1138–1141.
(15) Collin, J. P.; Guillerez, S.; Sauvage, J. P.; Barigelletti, F.; De Cola, L.; Flamigni, L.; Balzani, V. *Inorg. Chem.* **1991**, *30*, 4230–4238.
(16) Barigelletti, F.; Flamigni, L.; Balzani, V.; Collin, J.-P.; Sauvage, J.-P.; Sour, A.; Constable, E. C.; Thompson, A. M. W. C. *J. Am. Chem. Soc.* **1994**, *116*, 7692–7699.
(17) Beley, M.; Collin, J.-P.; Sauvage, J.-P.; Sugihara, H.; Heisel, F.; Miehe, A. *J. Chem. Soc., Dalton Trans.* **1991**, 3157–3159.
(18) Thummel, R. P.; Hegde, V.; Jahng, Y. *Inorg. Chem.* **1989**, *28*, 3264–3267.
(19) Maestri, M.; Armaroli, N.; Balzani, V.; Constable, E. C.; Thompson, A. M. W. C. *Inorg. Chem.* **1995**, *34*, 2759–2767.
(20) Abrahamsson, M.; Jager, M.; Osterman, T.; Eriksson, L.; Persson, P.; Becker, H. C.; Johansson, O.; Hammarstrom, L. *J. Am. Chem. Soc.* **2006**, *128*, 12616–12617.
(21) Abrahamsson, M.; Wolpher, H.; Johansson, O.; Larsson, J.; Kritikos, M.; Eriksson, L.; Norrby, P. O.; Bergquist, J.; Sun, L.; Akermark, B.; Hammarstrom, L. *Inorg. Chem.* **2005**, *44*, 3215–3225.
(22) Constable, E. C.; Harverson, P.; Smith, D. R.; Whall, L. *Polyhedron* **1997**, *16*, 3615–3623.
(23) Medlycott, E. A.; Hanan, G. S. *Coord. Chem. Rev.* **2006**, *250*, 1763–1782.
(24) Clarke, M. J. *Coord. Chem. Rev.* **2003**, *236*, 209–233.
(25) Farrer, B. T.; Thorp, H. H. *Inorg. Chem.* **2000**, *39*, 44–49.
(26) Grover, N.; Gupta, N.; Singh, P.; Thorp, H. H. *Inorg. Chem.* **1992**, *31*, 2014–2020.
(27) Chouai, A.; Wicke, S. E.; Turro, C.; Bacsa, J.; Dunbar, K. R.; Wang, D.; Thummel, R. P. *Inorg. Chem.* **2005**, *44*, 5996–6003.
(28) Liu, Y.; Hammitt, R.; Lutterman, D. A.; Thummel, R. P.; Turro, C. *Inorg. Chem.* **2007**, *46*, 6011–6021.
(29) Jain, A.; Slebodnick, C.; Winkel, B. S. J.; Brewer, K. J. *J. Inorg. Biochem.* **2008**, *102*, 1854–1861.
(30) Patel, K. K.; Plummer, E. A.; Darwish, M.; Rodger, A.; Hannon, M. J. *J. Inorg. Biochem.* **2002**, *91*, 220–229.
(31) Howe-Grant, M.; Lippard, S. J. *Biochemistry* **1979**, *18*, 5762–5769.
(32) Jiang, C.-W.; Chao, H.; Li, H.; Ji, L.-N. *J. Inorg. Biochem.* **2003**, *93*, 247–255.
(33) Ding, H.-Y.; Wang, X.-S.; Song, L.-Q.; Chen, J.-R.; Yu, J.-H.; Chao, L.; Zhang, B.-W. *J. Photochem. Photobiol., A* **2006**, *177*, 286–294.
(34) Milkevitch, M.; Shirley, B. W.; Brewer, K. J. *Inorg. Chim. Acta* **1997**, *264*, 249–256.
(35) Milkevitch, M.; Brauns, E.; Brewer, K. J. *Inorg. Chem.* **1996**, *35*, 1737–1739.

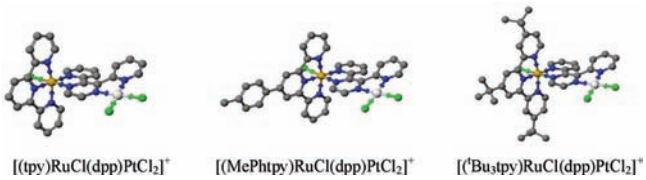

Figure 2. Mixed metal Ru(II)−Pt(II) complexes of the form TL−LA−BL−BAS with hydrogens omitted for clarity (TL = terminal ligand, LA = light absorber, BL = bridging ligand, BAS = bioactive site, tpy = 2,2′:6′,2″-terpyridine, MePhtpy = 4′-(4-methylphenyl)-2,2′:6′,2″-terpyridine, ^{t}Bu$_3$tpy = 4,4′,4″-tri-*tert*-butyl-2,2′:6′,2″-terpyridine), and dpp = 2,3-bis(2-pyridyl)pyrazine; gray sphere = carbon, blue sphere = nitrogen, green sphere = chlorine, gold sphere = ruthenium, and white sphere = platinum).

DNA through a *cis*-Pt^{II}Cl$_2$ moiety.[34] The positive charge imparted by the Ru(II) or Os(II) affords greater water solubility as well as increased electrostatic attraction toward DNA as compared to cisplatin.[34] The [(tpy)Ru(dtdeg)-PtCl]Cl$_3$ (dtdeg = bis[4′-(2,2′:6;2″-terpyridyl)]diethyleneglycol) complex has been reported to interact with DNA through intercalation in addition to covalent and electrostatic interactions.[36] Similarly, DNA−DNA and DNA−protein cross-linking interactions of the [(μ-NH$_2$(CH$_2$)$_4$NH$_2$){*cis*-Pt(NH$_3$)$_2$-Cl$_2$)}$_2$] complex have been reported.[37]

The DNA-binding properties of the heteronuclear bimetallic complexes, [(tpy)RuCl(BL)PtCl$_2$](PF$_6$) (BL = 2,3-bis-(2-pyridyl)pyrazine (dpp), 2,3-bis(2-pyridyl)quinoxaline (dpq), or 2,3-bis(2-pyridyl)benzoquinoxaline (dpb)), have been reported.[38] The [(tpy)RuCl(dpp)PtCl$_2$](PF$_6$) complex shows rapid binding to plasmid DNA with significant retardation of migration of the DNA through agarose gels as compared to that of cisplatin, though no photocleavage is reported. Brewer and co-workers have reported the Ru−Pt tetrametallic complex displaying covalent binding by a *cis*-Pt^{II}Cl$_2$ unit and DNA photocleavage via ruthenium polypyridyl moiety.[39] Recently, antimicrobial properties of the [(tpy)RuCl(dpp)PtCl$_2$](PF$_6$) complex have been reported.[40] Herman and co-workers have reported that the mixed metal supramolecular complex, consisting of a cisplatin moiety and two NAMI subunits [(ImH)(*trans*-RuCl$_4$(DMSO)-(Im))], is capable of DNA binding and potent against both neoplastic and metastatic cancer.[6]

Herein, we report the coupling of [(tpy)RuCl(BL)] subunits to a *cis*-Pt^{II}Cl$_2$ moiety, which provides for the application of typically shorter lived chromophores in DNA photocleavage applications. The impact of component modification on DNA-binding and photocleavage properties of Ru−Pt mixed metal supramolecular complexes is explored. With the proper choice of ligand, multifunctional supramolecular assemblies (Figure 2) can be formed that can coordinate to DNA through a *cis*-Pt^{II}Cl$_2$ moiety and can photocleave DNA through a tpy-containing Ru polyazine chromophore. These complexes exist as mixtures of two stereoisomers with the pyrazine of the dpp BL trans to the central pyridine ring of the tpy or the chloride ligand. The effect of subunit modification of the terminal tpy ligand upon spectroscopic and redox properties, DNA-binding, and DNA cleavage ability of the mixed metal supramolecular complexes is explored.

Experimental Section

Materials. All reagents were used as received unless otherwise noted. The ligands, 2,2′:6′,2″-terpyridine, 4′-(4-methylphenyl)-2,2′:6′,2″-terpyridine, 4,4′,4‴-tri-*tert*-butyl-2,2′:6′,2″-terpyridine, and 2,3-bis(2-pyridyl)pyrazine, were purchased from Aldrich Chemical Co. Ruthenium trichloride hydrate was obtained from Alfa Aesar. Adsorption alumina (80−200 mesh) was obtained from Fisher Scientific. Spectral grade acetonitrile was received from Burdick and Jackson. Circular plasmid pUC18 DNA was purchased from Bayou Biolab. Lambda DNA/*Hind*III molecular weight marker was obtained from Promega. Electrophoresis grade boric acid, agarose, and molecular biology grade glycerol were purchased from Fisher Scientific. The supporting electrolyte for electrochemical studies, tetrabutylammonium hexafluorophosphate (Bu_4NPF_6), was purchased from Fluka. The complexes, [(tpy)RuCl$_3$],[41] [(tpy)RuCl(dpp)](PF$_6$),[42] [(MePhtpy)RuCl$_3$],[41] [(MePhtpy)RuCl(dpp)](PF$_6$),[29] and [(^{t}Bu$_3$tpy)RuCl$_3$][43] were synthesized as previously reported.

Methods

ESI Mass Spectroscopy. Electrospray ionization mass spectral analysis was performed by M-Scan Inc., West Chester, PA, on a VG analytical ZA\B 2−SE high field mass spectrometer. The spectra observed for the complexes are consistent with the proposed molecular structure.

Electrochemistry. Cyclic and square wave voltammetric experiments were performed using a one compartment three-electrode cell, Epsilon potentiostat from Bioanalytical Systems (BAS). The three-electrode system consisted of a platinum disk working electrode, a platinum wire auxiliary electrode, and a Ag/AgCl reference electrode (0.21 V vs NHE). The reference electrode was calibrated using the $Fe(C_5H_5)_2/Fe(C_5H_5)_2^+$ couple (0.67 V vs NHE).[44] The supporting electrolyte used was 0.1 M Bu_4NPF_6, and measurements were carried out in spectral grade acetonitrile under argon.

Electronic Absorption Spectroscopy. Electronic absorption spectra were recorded at room temperature using a Hewlett-Packard 8452 diode array spectrophotometer with 2 nm resolution. Solutions were prepared gravimetrically in spectral grade acetonitrile, and data were collected at room temperature using 1 cm quartz cuvettes. The extinction coefficients are the average of three measurements on separate solutions.

DNA-Binding and Photocleavage Studies. The ability of the metal complex to bind and photocleave pUC18 plasmid DNA was assayed using agarose gel electrophoresis. All samples were prepared according to a standard protocol.[34] Master solutions of metal complexes were

(36) Schilden, K. V. D.; Garcia, F.; Kooijman, H.; Spek, A. L.; Haansoot, J. G.; Reedijk, J. *Angew. Chem., Int. Ed.* **2004**, *43*, 5668–5670.
(37) Houten, B. V.; Illenye, S.; Qu, Y.; Farrell, N. *Biochemistry* **1993**, *32*, 11794–11801.
(38) Williams, R. L.; Toft, H. N.; Winkel, B.; Brewer, K. J. *Inorg. Chem.* **2003**, *42*, 4394–4400.
(39) Miao, R.; Mongelli, M. T.; Zigler, D. F.; Winkel, B. S. J.; Brewer, K. J. *Inorg. Chem.* **2006**, *45*, 10413–10415.
(40) Jain, A.; Winkel, B. S. J.; Brewer, K. J. *J. Inorg. Biochem.* **2007**, *101*, 1525–1528.
(41) Sullivan, B. P.; Calvert, J. M.; Meyer, T. J. *Inorg. Chem.* **1980**, *19*, 1404–1407.
(42) Vogler, L. M.; Franco, C.; Jones, S. W.; Brewer, K. J. *Inorg. Chim. Acta* **1994**, *221*, 55–59.
(43) Hadda, T. B.; M., C.; Bozec, H. L. *Polyhedron* **1995**, *14*, 953–955.
(44) Gennett, T.; Milner, D. F.; Weaver, M. J. *J. Phys. Chem.* **1985**, *89*, 2787–2790.

prepared in 1% v/v aqueous DMSO:H_2O. Stock solutions (2 mL) were made to have ~1% DMSO, pUC18 DNA (15.3 μM (BP)) and 0.76 μM metal complex (MC) (to achieve 20:1 BP to MC) in 10 mM NaH_2PO_4 buffer (pH 7). Prior to photolysis, half of the stock solution was deoxygenated by bubbling with argon for 20 min. The samples were irradiated with light from a 1000 W xenon arc lamp equipped with a water IR filter and a 450 nm cutoff filter. Small aliquots of the solutions (10 μL containing 0.1 μg of DNA) were mixed with 2 μL glycerol-based gel loading buffer and loaded into the wells of a gel made with 0.8% w/w agarose, 0.55% w/w boric acid, and 1.08% w/w tris base. Electrophoresis was performed using an Owl Separation Systems, Inc. (Portsmouth, NH) Model B1A electrophoresis stage at 104 V (~35 mA) for 1.5 h. Gels were stained with 0.5 μg/mL ethidium bromide for 45 min followed by 45 min of destaining in ddH_2O. Gels were visualized on a Fisher Biotech UV transilluminator. Photographs were taken using an Olympus E-320 digital camera equipped with a Peca Products Inc. ethidium bromide filter.

Synthesis

[(tpy)RuCl(dpp)$PtCl_2$](PF_6). [(tpy)RuCl(dpp)$PtCl_2$](PF_6) was prepared using a slight modification of the published method.[38] The [(tpy)RuCl(dpp)](PF_6)[42] (300 mg, 0.40 mmol) and the [$PtCl_2(DMSO)_2$][45] (250 mg, 0.60 mmol) were heated at reflux in 10 mL of 95% ethanol. During the 1 h reaction time, the solution changed from red to purple. Once the reaction mixture had cooled to room temperature, the purple product precipitated and was separated by vacuum filtration on a fine-porosity fritted funnel. The product was washed with two 10 mL portions of ethanol and 10 mL of chloroform. The product obtained was purified using hot ethanol recrystallization. The solid was redissolved in ca. 15 mL of CH_3CN and filtered. The product was then flash precipitated by addition of 60 mL of stirring diethyl ether. Yield: 90% (360 mg, 0.36 mmol). Electrospray ionization mass spectrometry of [(tpy)RuCl(dpp)$PtCl_2$](PF_6) was consistent with its formulation. (m/z; relative abundance): [(tpy)RuCl(dpp)$PtCl_2$]$^+$ (870, 100); [(tpy)RuCl(dpp)PtCl]$^+$ (834, 10) (δ^{195}Pt = −2 199).

[(MePhtpy)RuCl(dpp)$PtCl_2$](PF_6). [(MePhtpy)RuCl(dpp)$PtCl_2$](PF_6) was prepared by a modification of the method used for [(tpy)RuCl(dpp)$PtCl_2$](PF_6)[38] using [(MePhtpy)RuCl(dpp)](PF_6) (330 mg, 0.40 mmol). The resulting purple product was purified by hot ethanol recrystallization. Yield: 84% (400 mg, 0.34 mmol). Electrospray ionization mass spectrometry of [(MePhtpy)RuCl(dpp)$PtCl_2$](PF_6) was consistent with its formulation complex. (m/z; relative abundance): [(MePhtpy)RuCl(dpp)$PtCl_2$]$^+$ (960, 40); [(MePhtpy)RuCl(dpp)PtCl]$^+$ (924, 18); [(MePhtpy)RuCl(dpp)]$^+$ (694, 100) (δ^{195}Pt = −2 201).

[(^{t}Bu$_3$tpy)RuCl(dpp)$PtCl_2$](PF_6). [(^{t}Bu$_3$tpy)RuCl(dpp)$PtCl_2$](PF_6) was prepared by a modification of the method used for [(tpy)RuCl(dpp)$PtCl_2$](PF_6)[38] using [(^{t}Bu$_3$tpy)RuCl(dpp)](PF_6) (360 mg, 0.40 mmol). The resulting purple product was purified by hot ethanol recrystallization. Yield: 72% (340 mg, 0.29 mmol). Electrospray ionization mass spectrometry of [(^{t}Bu$_3$tpy)RuCl(dpp)$PtCl_2$](PF_6) was consistent with its formulation complex. (m/z; relative abundance): [(^{t}Bu$_3$tpy)RuCl(dpp)$PtCl_2$]$^+$ (1 038, 100); [(^{t}Bu$_3$tpy)RuCl(dpp)PtCl]$^+$ (1 002, 10) (δ^{195}Pt = −2 220).

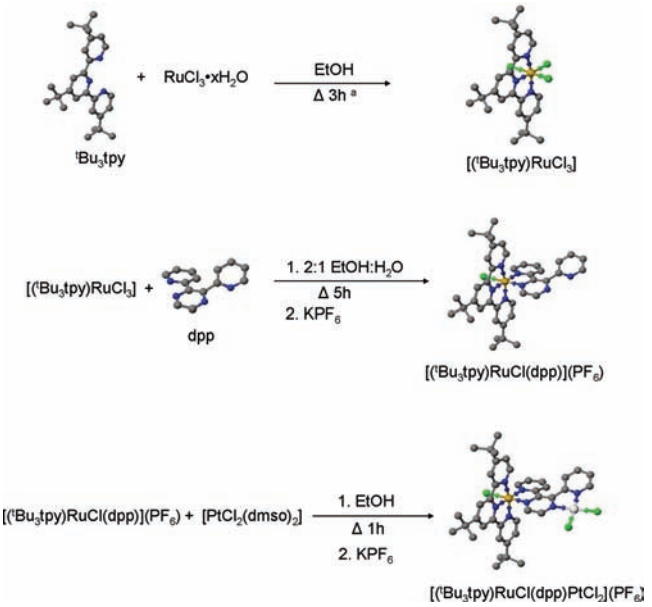

Figure 3. Building block method used to prepare mixed metal supramolecular complexes (^{t}Bu$_3$tpy = 4,4′,4″-tri-*tert*-butyl-2,2′:6′,2″-terpyridine), and dpp = 2,3-bis(2-pyridyl)pyrazine). Adapted from ref 43.

Results and Discussion

Metal complexes of the type TL−LA−BL−BAS (TL = terminal ligand, LA = light absorber, BL = bridging ligand, and BAS = bioactive site) were prepared, and their basic chemical properties as well as ground- and excited-state interactions with DNA were studied. The membrane permeability of these metal complexes was varied by addition of different substituents on the terminal tpy ligand. The building block approach was used to synthesize the bimetallic complexes in good yield (Figure 3). The building block method allows for construction of this molecular architecture by first binding the terminal ligand, tpy, to the ruthenium metal center followed by attachment of the bridging ligand, dpp. The Pt^{II} coordination is achieved in the final step. These complexes contain a tunable light-absorbing unit and a *cis*-$Pt^{II}Cl_2$ moiety. Herein, the variation in the light absorbing unit was achieved by changing the substituents on the tridentate terminal ligand. The light-absorbing unit contains chloride in its sixth coordination site. These metal complexes have been characterized by ESI MS spectral analysis, and the fragmentation pattern observed was consistent with the formulation of these complexes. ^{1}H NMR is complicated due to the presence of two isomers about the Ru center. ^{195}Pt NMR data show a single but broadened resonance for each complex consistent with the proposed structures.

Electrochemistry. Electrochemistry is used to understand the energetics associated with the redox process and the frontier orbitals in the Ru(II)−Pt(II) mixed metal complexes. Ruthenium polypyridyl complexes typically display reversible Ru-based oxidations and a series of reversible ligand-based reductions. The heteronuclear bimetallic complexes and the previously reported

(45) Sahai, R.; Rillema, D. P. *J. Chem. Commun.* **1986**, 1133–1134.

Table 1. Cyclic Voltammetric Data for $[(TL)RuCl(dpp)PtCl_2](PF_6)$ and Monometallic Synthons[a]

metal complex	$E_{1/2}^{ox}$(V)[b]	$E_{1/2}^{red}$(V)[b]
$[(tpy)RuCl(dpp)PtCl_2](PF_6)$[c]	+1.10 $Ru^{II/III}$	−0.50 $dpp^{0/-}$ −1.15 $dpp^{-/2-}$ −1.43 $tpy^{0/-}$
$[(MePhtpy)RuCl(dpp)PtCl_2](PF_6)$	+1.10 $Ru^{II/III}$	−0.55 $dpp^{0/-}$ −1.20 $dpp^{-/2-}$ −1.44 $MePhtpy^{0/-}$
$[(^tBu_3tpy)RuCl(dpp)PtCl_2](PF_6)$	+1.01 $Ru^{II/III}$	−0.59 $dpp^{0/-}$ −1.15 $dpp^{-/2-}$ −1.59 $^tBu_3tpy^{0/-}$
$[(tpy)RuCl(dpp)](PF_6)$[d]	+1.02 $Ru^{II/III}$	−1.15 $dpp^{0/-}$ −1.41 $tpy^{0/-}$
$[(MePhtpy)RuCl(dpp)](PF_6)$[e]	+1.01 $Ru^{II/III}$	−1.16 $dpp^{0/-}$ −1.40 $MePhtpy^{0/-}$
$[(^tBu_3tpy)RuCl(dpp)](PF_6)$	+0.98 $Ru^{II/III}$	−1.22 $dpp^{0/-}$ −1.59 $^tBu_3tpy^{0/-}$

[a] TL = terminal ligand (tpy = 2,2′:6′,2″-terpyridine, MePhtpy = 4′-(4-methylphenyl)-2,2′:6′,2″-terpyridine, $^tBu_3tpy$ = 4,4′,4″-tri-*tert*-butyl-2,2′:6′,2″-terpyridine) and dpp = 2,3-bis(2-pyridyl)pyrazine. [b] Potential reported in CH_3CN with 0.1 M Bu_4NPF_6 and reported vs Ag/AgCl (0.21 V vs NHE) reference electrode. [c] Redox potentials recorded under our conditions are consistent with the previous report.[38] [d] Redox potentials recorded under our conditions are consistent with the previous report.[42] [e] Redox potentials recorded under our conditions are consistent with the previous report.[29]

monometallic precursors have been studied by cyclic voltammetry, and the data are summarized in Table 1. Cyclic voltammograms for the title $[(TL)RuCl(dpp)PtCl_2](PF_6)$ systems in 0.1 M Bu_4NPF_6 in CH_3CN are shown in Figure 4.

The heterobimetallic complexes display electrochemistry consistent with their formulation. These complexes display reversible $Ru^{II/III}$ oxidation, establishing the Ru metal center as a site for the localization of the HOMO. The $Ru^{II/III}$ oxidation in the $[(tpy)RuCl(dpp)PtCl_2](PF_6)$[38] and $[(MePhtpy)RuCl(dpp)PtCl_2](PF_6)$ complexes occurred at 1.10 V vs Ag/AgCl, which is shifted to a more positive potential relative to the monometallic synthons. The $Ru^{II/III}$ oxidation couple occurs at a less positive potential in $[(^tBu_3tpy)RuCl(dpp)PtCl_2](PF_6)$ complex compared to the other two heterobimetallic complexes. This lowering of the oxidation potential results from the electron-donating character of the $^tBu_3$ group, making the Ru center more electron rich and, therefore, easy to oxidize. A similar effect was reported by Hadda and LeBoez with a 75 mV decrease in the potential when $^tBu_3tpy$ and $^tBu_3bpy$ were substituted for tpy and bpy, respectively, in $[Ru(^tBu_3tpy)Cl(bpy)]^+$ and $[Ru(^tBu_3bpy)Cl(tpy)]^+$.[46,47] Each $[(TL)RuCl(dpp)PtCl_2](PF_6)$ complex displays a reversible $dpp^{0/-}$-based first reduction, establishing the BL as a site of localization of LUMO for these heterobimetallic complexes. This $dpp^{0/-}$ couple is ca. 0.60 V more positive in the bimetallic complexes compared to the monometallic synthons

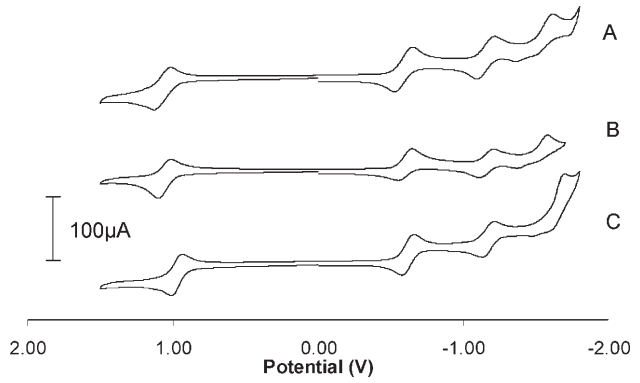

Figure 4. Cyclic voltammograms of $[(tpy)RuCl(dpp)PtCl_2](PF_6)$ (A), $[(MePhtpy)RuCl(dpp)PtCl_2](PF_6)$ (B), and $[(^tBu_3tpy)RuCl(dpp)PtCl_2](PF_6)$ (C) in 0.1 M Bu_4NPF_6 in CH_3CN and reported vs Ag/AgCl (TL = terminal ligand (tpy = 2,2′:6′,2″-terpyridine, MePhtpy = 4′-(4-Methylphenyl)-2,2′:6′,2″-terpyridine, $^tBu_3tpy$ = 4,4′,4″-tri-*tert*-butyl-2,2′:6′,2″-terpyridine), dpp = 2,3-bis(2-pyridyl)pyrazine).

Scheme 1. Electrochemical Mechanism for $[(TL)RuCl(dpp)PtCl_2](PF_6)$ with Synthesized Oxidation State in Bold[a]

$$[(TL)Ru^{III}Cl(dpp)Pt^{II}Cl_2]^{2+}$$
$$-1e^- \rightleftharpoons +1e^-$$
$$\mathbf{[(TL)Ru^{II}Cl(dpp)Pt^{II}Cl_2]^{+}}$$
$$-1e^- \rightleftharpoons +1e^-$$
$$[(TL)Ru^{II}Cl(dpp^{-})Pt^{II}Cl_2]$$
$$-1e^- \rightleftharpoons +1e^-$$
$$[(TL)Ru^{II}Cl(dpp^{2-})Pt^{II}Cl_2]^{-}$$
$$-1e^- \rightleftharpoons +1e^-$$
$$[(TL^{-})Ru^{II}Cl(dpp^{2-})Pt^{II}Cl_2]^{2-}$$

[a] TL = terminal ligand (tpy = 2,2′:6′,2″-terpyridine, MePhtpy = 4′-(4-methylphenyl)-2,2′:6′,2″-terpyridine, $^tBu_3tpy$ = 4,4′,4″-tri-*tert*-butyl-2,2′:6′,2″-terpyridine) and dpp = 2,3-bis(2-pyridyl)pyrazine).

consistent with the significant stabilization of the dpp (π^*) LUMO upon complexation to the Pt^{II} center.[48] The second reduction in the bimetallic complexes is $dpp^{-/2-}$ in nature, indicative of a bridging dpp. Stabilization of the dpp (π^*) acceptor orbital, as a result of the coordination to the *cis*-$Pt^{II}Cl_2$ moiety, shifts this $dpp^{-/2-}$ couple positive to the $TL^{0/-}$ couple. The third reduction in these metal complexes is $TL^{0/-}$ in nature. The reduction of tpy and MePhtpy in these heterobimetallic complexes occurred at −1.40 and −1.46 V. The reduction of the $^tBu_3tpy$ occurs at a more negative potential, −1.59 V, due to the electron-donating character of $^tBu_3$ group. Scheme 1 summarizes the electrochemical mechanism for these heterobimetallic complexes.

Electronic Absorption Spectroscopy. The electronic absorption spectra of heterobimetallic complexes of the form $[(TL)RuCl(dpp)PtCl_2](PF_6)$ in acetonitrile are shown in Figure 5. All the heterobimetallic complexes are efficient light absorbers with the spectrum dominated by TL−LA−BL subunit. Ruthenium polyazine complexes display a ligand-based $\pi \rightarrow \pi^*$ transition in the UV region and a MLCT transition in the visible region,

(46) Hadda, T. B.; Bozec, H. L. *Polyhedron* **1988**, *7*, 575–578.
(47) Hadda, T. B.; Bozec, H. L. *Inorg. Chim. Acta* **1993**, *204*, 103–107.
(48) Swavey, S.; Williams, R. L.; Fang, Z.; Milkevitch, M.; Brewer, K. J. *Proc. SPIE-Int. Soc. Opt. Eng.* **2001**, *4512*, 75–83.

terminating in each acceptor ligand. The spectra of all the complexes displayed intense TL-based $\pi\rightarrow\pi^*$ transitions in the UV region with the two major peaks at 272 and 316 nm attributed to the tpy ligand. The dpp-based $\pi\rightarrow\pi^*$ transition occurred at a lower energy as a shoulder at ca. 354 nm. These complexes display an intense MLCT band in the visible region of the spectrum. The Ru→TL charge transfer band occurs at a higher energy than the Ru→dpp charge transfer band and is centered at ca. 460 nm for all three complexes.

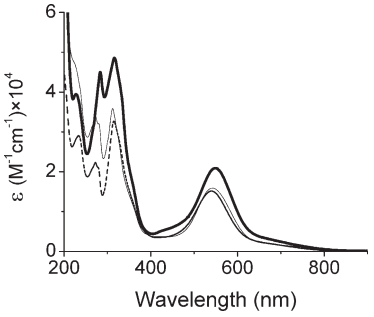

Figure 5. Electronic absorption spectroscopy of [(tpy)RuCl(dpp)-$PtCl_2$](PF_6) (···), [(MePhtpy)RuCl(dpp)$PtCl_2$](PF_6) (—) and [(^{t}Bu$_3$tpy)-RuCl(dpp)$PtCl_2$](PF_6) (—) in CH_3CN at room temperature (tpy = 2,2′:6′,2″-terpyridine, MePhtpy = 4′-(4-methylphenyl)-2,2′:6′,2″-terpyridine, ^{t}Bu$_3$tpy = 4,4′,4″-tri-*tert*-butyl-2,2′:6′,2″-terpyridine), and dpp = 2,3-bis(2-pyridyl)pyrazine).

The Ru→dpp CT band was centered at 540 nm and is red shifted ca. 20 nm in the bimetallic complexes relative to the corresponding [(TL)RuCl(dpp)](PF_6) monometallic synthons. This red shift is due to the stabilization of the dpp π^* orbitals by coordination to the electropositive Pt(II) metal center and is consistent with the electrochemical results. The electronic absorption spectral properties of [(TL)RuCl(dpp)$PtCl_2$](PF_6) complexes and their monometallic synthons are summarized in Table 2.

DNA-Binding Studies. The DNA-binding ability of the heterobimetallic complexes, [(TL)RuCl(dpp)$PtCl_2$](PF_6), was explored using agarose gel electrophoresis. These metal complexes contain a *cis*-$Pt^{II}Cl_2$ moiety, which is known to covalently bind to DNA and is the basis of a class of anticancer agents. Figure 6 shows the gel electrophoresis study of these complexes compared to the standard, cisplatin, using linear pUC18 DNA. In this study, each metal complex was combined with linearized pUC18 DNA at a range of base pair (BP) to metal complex (MC) ratios. These mixtures were incubated for 1 h at 37 °C and analyzed by agarose gel electrophoresis as shown in Figure 6. Lane λ (one), is the molecular weight standard (24, 9.4, 6.6, 4.4, 2.2, and 2.0 kb), lane C (two) is the pUC18 DNA control without any metal complex present, lane 5:1 (three) is the pUC18 DNA incubated with 5:1 BP:MC, lane 10:1 (four) is the pUC18 DNA incubated with 10:1 BP:MC, and lane 20:1 (five) is the pUC18 DNA

Table 2. Electronic Absorption Spectroscopy for [(TL)RuCl(dpp)$PtCl_2$](PF_6) and Related Monometallic Synthons in CH_3CN at Room Temperature[a]

complex	λ_{max}^{abs} (nm)	$\varepsilon \times 10^{-4}$ ($M^{-1}cm^{-1}$)	assignment
[(tpy)RuCl(dpp)$PtCl_2$](PF_6)[b]	236	2.87	$\pi\rightarrow\pi^*$ tpy
	317	3.22	$\pi\rightarrow\pi^*$ tpy
	354(sh)	1.40	$\pi\rightarrow\pi^*$ dpp
	462(sh)	0.490	Ru→tpy CT
	544	1.53	Ru→dpp CT
[(MePhtpy)RuCl(dpp)$PtCl_2$](PF_6)	227	4.67	$\pi\rightarrow\pi^*$ MePhtpy
	318	4.82	$\pi\rightarrow\pi^*$ MePhtpy
	354(sh)	1.90	$\pi\rightarrow\pi^*$ dpp
	464(sh)	0.670	Ru→MePhtpy CT
	548	2.09	Ru→dpp CT
[(^{t}Bu$_3$tpy)RuCl(dpp)$PtCl_2$](PF_6)	230	3.92	$\pi\rightarrow\pi^*$ ^{t}Bu$_3$tpy
	314	3.53	$\pi\rightarrow\pi^*$ ^{t}Bu$_3$tpy
	354(sh)	1.42	$\pi\rightarrow\pi^*$ dpp
	462(sh)	0.490	Ru→^{t}Bu$_3$tpy CT
	545	1.54	Ru→dpp CT
[(tpy)RuCl(dpp)](PF_6)[c]	237	3.40	$\pi\rightarrow\pi^*$ tpy
	315	4.60	$\pi\rightarrow\pi^*$ tpy
	364(sh)	0.680	$\pi\rightarrow\pi^*$ dpp
	516	1.43	Ru→dpp CT
			Ru→tpy CT
[(MePhtpy)RuCl(dpp)](PF_6)	228	3.32	$\pi\rightarrow\pi^*$ MePhtpy
	312	4.32	$\pi\rightarrow\pi^*$ MePhtpy
	356(sh)	0.610	$\pi\rightarrow\pi^*$ dpp
	522	1.72	Ru→dpp CT
			Ru→MePhtpy CT
[(^{t}Bu$_3$tpy)RuCl(dpp)](PF_6)	240	4.20	$\pi\rightarrow\pi^*$ ^{t}Bu$_3$tpy
	314	5.02	$\pi\rightarrow\pi^*$ ^{t}Bu$_3$tpy
	360(sh)	0.801	$\pi\rightarrow\pi^*$ dpp
	521	1.53	Ru→dpp CT
			Ru→^{t}Bu$_3$tpy CT

[a] TL = terminal ligand (tpy = 2,2′:6′,2″-terpyridine, MePhtpy = 4′-(4-methylphenyl)-2,2′:6′,2″-terpyridine, ^{t}Bu$_3$tpy = 4,4′,4″-tri-*tert*-butyl-2,2′:6′,2″-terpyridine) and dpp = 2,3-bis(2-pyridyl)pyrazine. [b] Extinction coefficients recorded under our conditions are consistent with the previous report.[38] [c] Extinction coefficients recorded under our conditions are consistent with the previous report.[42]

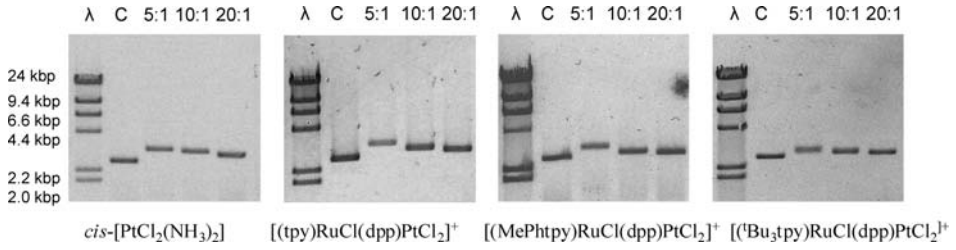

Figure 6. DNA-binding study for $[(TL)RuCl(dpp)PtCl_2](PF_6)$ by agarose gel electrophoresis using linearized pUC18 DNA (dpp = 2,3-bis(2-pyridyl)pyrazine, TL = terminal ligand (tpy = 2,2′:6′,2″- terpyridine, MePhtpy = 4′-(4-methylphenyl)-2,2′:6′,2″-terpyridine, and ^{t}Bu$_3$tpy = 4,4′,4″-tri-*tert*-butyl-2,2′:6′,2″-terpyridine). λ is the molecular weight standard (24, 9.4, 6.6, 4.4, 2.3, and 2.0 kbp), C is the DNA control, 5:1 is the 5:1 base pairs (BP): metal complex (MC) ratio, 10:1 is the 10:1 BP:MC ratio, and 20:1 is the 20:1 BP:MC ratio.

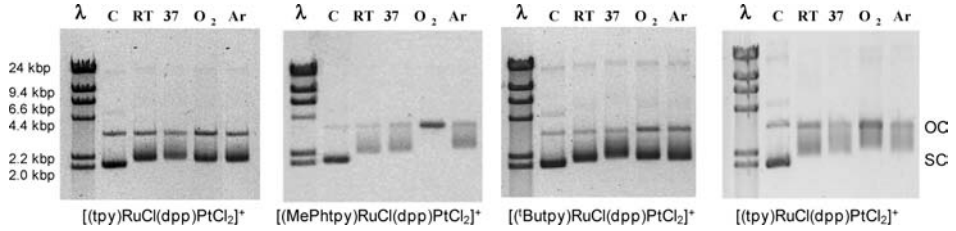

Figure 7. DNA-binding and photocleavage study for $[(TL)RuCl(dpp)PtCl_2](PF_6)$ by agarose gel electrophoresis using circular pUC18 DNA (dpp = 2,3-bis(2-pyridyl)pyrazine, TL = terminal ligand (tpy = 2,2′:6′,2″-terpyridine, MePhtpy = 4′-(4-methylphenyl)-2,2′:6′,2″-terpyridine, ^{t}Bu$_3$tpy = 4,4′,4″-tri-*tert*-butyl-2,2′:6′,2″-terpyridine). λ is the molecular weight standard (24, 9.4, 6.6, 4.4, 2.3, and 2.0 kbp), C is the DNA control, RT is the 20:1 BP:MC incubated at room temperature for 2 h, 37 is the 20:1 BP:MC incubated at 37 °C for 2 h, O_2 is the 20:1 base pair (BP): metal complex (MC) photolyzed with 450−1000 nm light for 2 h under atmospheric conditions, and Ar is the 20:1 BP:MC photolyzed with 450−1000 nm light for 2 h in the absence of oxygen. The $[(tpy)RuCl(dpp)PtCl_2]^+$ on the right is incubated and photolyzed for 4 h with other conditions remaining the same.

incubated with 20:1 BP:MC. Cisplatin is known to form coordinate covalent bonds with DNA, and this can be visualized in the gel as a decrease in DNA migration through the gel, with the increase of MC concentration moving from lane 20:1 to 10:1 to 5:1. The $[(tpy)RuCl(dpp)PtCl_2](PF_6)$[40] and $[(MePhtpy)RuCl(dpp)PtCl_2](PF_6)$ complexes exhibited coordinate covalent binding to DNA with a significant retardation of pUC18 DNA migration through the gel and a greater effect at lower BP:MC ratios. The reduction of the DNA migration through the gel was found to be greater for these two complexes as compared to that of cisplatin. The R_f values compared to the 2.0 kb λ control were calculated at a 5:1 BP:MC ratio and found to be 0.68 (cisplatin), 0.62 ($[(tpy)RuCl(dpp)PtCl_2](PF_6)$), 0.64 ($[(MePhtpy)RuCl(dpp)PtCl_2](PF_6)$), and 0.74 ($[(^tBu_3tpy)RuCl(dpp)PtCl_2](PF_6)$) relative to 0.80 for the DNA control. These types of metal complexes and cisplatin have been shown to bind with the guanine (G-7) base of DNA.[34] The $[(^tBu_3tpy)RuCl(dpp)PtCl_2](PF_6)$ complex displayed somewhat less effect on DNA migration through the agarose gel. The introduction of the $^tBu_3$ groups on the terpyridine ligand makes the molecule sterically hindered relative to the unsubstituted tpy-containing complex and provides a lipophilic site remote from the *cis*-$Pt^{II}Cl_2$ site. It may be sterically difficult for *cis*-$Pt^{II}Cl_2$ subunits of this metal complex to reach the G-7 of DNA. Baguely and co-workers have also shown that the presence of bulky groups lowers the DNA binding and cytotoxicity of amsacrine.[49] The monometallic synthons have been previously assayed for DNA interactions for TL = tpy and MePhtpy and are not found to thermally bind DNA, such as to impact electrophoretic mobility as is typical of most Ru polyazine complexes.[29] Ionic and intercalative binding of cationic Ru polyazine complexes is typically not stable under electrophoresis, and in fact, the monometallic systems are typically observed migrating in the opposite direction of the DNA due to their positive charge.

DNA Photocleavage Studies. The ability of the heterobimetallic complexes to photocleave DNA was studied by agarose gel electrophoresis using circular plasmid pUC18 DNA (Figure 7). In this study metal complexes were combined with pUC18 DNA at a 20:1 BP:MC ratio. The mixtures were irradiated with visible light ($\lambda_{irr} \geq$ 450−1000 nm) for 2 h, and the ability to photocleave DNA was analyzed by gel electrophoresis. In each panel, λ is the molecular weight standard, C is the DNA control showing that pUC18 exists mostly in the supercoiled state together with a small amount of nicked circular DNA, RT is the DNA incubated with the metal complex in the dark at room temperature, 37 is the DNA incubated with the metal complex in the dark at 37 °C, O_2 is the DNA and metal complex irradiated with 450−1000 nm light for 2 h under atmospheric conditions, and Ar is the DNA and metal complex irradiated with 450−1000 nm light for 2 h under argon. The complexes $[(tpy)RuCl(dpp)PtCl_2]^+$ and $[(^tBu_3tpy)RuCl(dpp)PtCl_2]^+$ were also assayed at 4 h of incubation and photolysis. No changes were observed for the $[(^tBu_3tpy)RuCl(dpp)PtCl_2]^+$, so it is not shown.

The gel electrophoresis studies using circular plasmid pUC18 DNA show that the three metal complexes bind to DNA at room temperature or upon 37 °C incubation (RT and 37 lanes in the first two gels in Figure 7) and photocleave DNA upon visible light irradiation (lanes O_2 in Figure 7). The observed DNA binding in lanes RT and 37 are consistent with the DNA-binding studies using linear pUC18 DNA (Figure 6). The $[(^tBu_3tpy)RuCl(dpp)PtCl_2](PF_6)$ metal complex displayed reduced covalent

(49) Denny, W. A.; Twigden, S. J.; Baguley, B. C. *Anti-Cancer Drug Des.* **1986**, *1*, 125–132.

binding to DNA upon thermal and room temperature incubation as compared to that of the tpy analog. Similar effects were observed in the DNA-binding studies using linear pUC18 DNA. Photolysis under oxygenated conditions yielded DNA photocleavage in the presence of [(tpy)RuCl(dpp)$PtCl_2$](PF_6) and [(MePhtpy)RuCl(dpp)-$PtCl_2$](PF_6), with most efficient conversion of the supercoiled form into the open circular form in the presence of [(MePhtpy)RuCl(dpp)$PtCl_2$](PF_6). The [(MePhtpy)RuCl(dpp)$PtCl_2$](PF_6) is a remarkably efficient DNA photocleavage agent, leading to complete conversion of the SC pUC18 to the OC form in 2 h photolysis at a low 20:1 BP:MC ratio. Minimal to no photocleavage was observed in the presence of the [(^{t}Bu$_3$tpy)RuCl(dpp)$PtCl_2$](PF_6) metal complex even when photolyzed for 4 h. The [(tpy)RuCl(dpp)$PtCl_2$](PF_6) complex binds to DNA to a larger extent when incubated for 4 h and cleaves DNA more when photolyzed for 4 h, Figure 7 far right gel. This is consistent with thermal binding by the Pt center being enhanced at longer times, and the cleavage of DNA through photosensitization of O_2 by the Ru LA unit is more efficient. Minor changes are seen when the [(MePhtpy)RuCl-(dpp)$PtCl_2$](PF_6) is photolyzed under Ar potentially indicative of minor photobinding of this complex.

The trend in the DNA photocleavage ability of these complexes with TL variation shows the MePhtpy complex to be an efficient DNA cleavage agent with the tpy system significantly less functional and the ^{t}Bu$_3$tpy system largely inactive. The log *P* values were determined to assay lipophilicity of the complexes by the shake flask method using water and octanol. The log *P* values were found to be −2.00, −0.39, and 4.00 for [(tpy)RuCl(dpp)-$PtCl_2$]Cl, [(MePhtpy)RuCl(dpp)$PtCl_2$]Cl, and [(^{t}Bu$_3$tpy)-RuCl(dpp)$PtCl_2$]Cl, respectively, showing the highest degree of octanol partitioning for the ^{t}Bu$_3$tpy complex. The lipophilc nature of the Bu$_3$tpy ligand and/or the steric hindrance in the molecule may prevent Pt complexation to the DNA, which would inhibit DNA photocleavage. Baguely and co-workers have demonstrated that by increasing the bulk of the group on the acridine moiety of amsacrine from methyl to ethyl and isopropyl, the intercalative binding to DNA was retained, but the apparent unwinding angle was lowered to about 30% by the isopropyl.[49] In the presence of the *t*-butyl group, they observed abrupt change to a nonintercalative binding from the intercalative binding mode.[49] The bimetallic complexes do not display a detectable emission from their ^{3}MLCT excited states likely due to the low energy of these states. The previously reported emission from the monometallic synthons [(tpy)RuCl(dpp)](PF_6) and [(MePhtpy)RuCl(dpp)](PF_6) shows little difference in their excited-state properties, τ = 17 and 16 ns, respectively, with similar emission quantum yields.[29] This suggests the rate of O_2 quenching in the bimetallic complexes is likely similar making somewhat surprising that the [(MePhtpy)RuCl(dpp)$PtCl_2$](PF_6) complex has a significantly larger degree of DNA photocleavage in this bimetallic framework.

The ability to modulate DNA reactivity by enhancing photocleavage with a MePhtpy ligand while impairing photocleavage with a ^{t}Bu$_3$tpy ligand within a bimetallic framework is unprecedented. The ability of the Pt coordination to provide for efficient DNA photocleavage to Ru^{II}tpy-containing chromophores provides for the application of this class of generally unexplored light absorbers for DNA photochemistry.

Conclusions

A series of multifunctional mixed metal supramolecular complexes of the type [(TL)Ru(dpp)$PtCl_2$](PF_6) with varying terminal ligands have been successfully synthesized using a building block method, and they are shown to display multifunctional interactions with DNA. These metal complexes display reversible $Ru^{II/III}$-based oxidation and $dpp^{0/-}$- and $dpp^{-/2-}$-based reductions prior to the $TL^{0/-}$-based reduction with only small variations in potential through the series of complexes. The tpy-based reduction in the [(^{t}Bu$_3$tpy)RuCl-(dpp)$PtCl_2$](PF_6) complex occurred at a more negative potential relative to those in the other two complexes due to the electron-donating nature of the ^{t}Bu$_3$ group. These complexes display Ru→dpp charge transfer bands in the visible region of the spectrum with tails at lower energy with all three complexes displaying similar and efficient light absorbing properties. The coupling of the cisplatin unit to a ruthenium-based chromophore provides not only the *cis*-$Pt^{II}Cl_2$ coordinate covalent DNA-binding ability but also the spectroscopic probe and photoactivity of these supramolecules. The [(tpy)RuCl(dpp)$PtCl_2$](PF_6) and [(MePhtpy)RuCl(dpp)$PtCl_2$](PF_6) complexes avidly bind to DNA and cleave DNA by molecular oxygen sensitization through the ^{3}MLCT state of the Ru polyazine unit, representing one of only a handful of multifunctional DNA-binding and photocleaving agents. The [(^{t}Bu$_3$tpy)RuCl(dpp)$PtCl_2$]-(PF_6) complex displays minimal coordinate covalent binding to DNA compared to the other two complexes. The presence of the ^{t}Bu$_3$ group on the terpyridine moiety lowers Pt coordination to the DNA. The presence of the methylphenyl group on the tpy ligand improves the interaction of the molecule with DNA, providing more facile DNA binding and photocleavage. With careful selection of the substitutents on the ligands, the DNA interaction properties of the molecules can be improved, and efficient multifunctional molecules can be designed. Work is currently in progress to explore these and related systems in detail to derive structure activity relationships.

Acknowledgment. The authors thank the National Science Foundation (CHE-0408445) for their generous support of this research and Ms. Samantha Hopkins for her assistance with this work.